Thermal Property of an Octadecyldimethylamine Oxide Multilayer Langmuir−Blodgett Film Studied by an Expanded Model for Quantitative Molecular Orientation Analysis with Infrared Reflection−Absorption Spectrometry

T. Hasegawa,*,† D. A. Myrzakozha,‡ T. Imae,§ J. Nishijo,† and Y. Ozaki‡

Kobe Pharmaceutical University, Motoyama-kita, Higashinada-ku, Kobe 658-8558, Japan, School of Science, Kwansei Gakuin University, Nishinomiya 662-8501, Japan, and Research Center for Materials Science, Nagoya University, Chikusa-ku, Nagoya 464-8602, Japan

Received: July 9, 1999; In Final Form: September 18, 1999

The thermal property of octadecyldimethylamine oxide (C_{18}DAO) multilayer Langmuir−Blodgett (LB) film was investigated by infrared reflection−absorption (IRRA) spectrometry and two techniques of molecular orientation analysis. A conventional estimation theory of molecular orientation is expanded in the present study so that the first layer of the LB film that shows thermal properties significantly different from other layers is discussed separately. The results by the conventional analytical technique suggest that the multilayer LB film is thermally disordered at 50 °C and melts at 60 °C. The new technique, on the other hand, suggests that only the first layer of the LB film is greatly disordered between 50 and 60 °C, prior to the entire melting above 60 °C. The newly proposed technique gives insight into the structure of a LB film that is not uniform in structure that depends on thickness. The differing of thermal properties of the first and the rest of the layers revealed by the new method suggests that the headgroup of C_{18}DAO has a uniquely strong interaction potential with the gold surface, probably due to its strong dipole.

Introduction

Two-dimensional molecular assemblies are accepting various interests,[1−10] since they possess unique physical or chemical properties that are not found in bulk aggregates and crystals. The unique properties are often found in biological systems. Phospholipids are, for example, known to form stable bilayers, which construct cell walls.[11−13] The physical property and function of the bilayers often reflect molecular structural differences particularly found in the vicinity of the headgroup of the phospholipid,[14] while they also reflect the chain length of hydrocarbon chains in the phospholipid.

This structure dependence reminds us of an idea that a new two-dimensional assembly of a designed molecule may have a novel unique property that is not found in nature. Hydrogen bonding studies of artificially synthesized molecules with the use of the Langmuir−Blodgett (LB) technique may be good examples.[9,15,16] That is why, in recent years, comprehensive studies from molecular design to structural and functional analyses of monolayer films are extensively undertaken.

Octadecyldimethylamine oxide (C_{18}DAO: Chart 1) is a molecule of interest as a detergent, since its headgroup is small and its dipole moment is uniquely strong.[17−23] Although the headgroup is small, C_{18}DAO is known to form a stable monolayer film at an air−water interface (Langmuir (L) film).[18,22] Since the molecule has a single long hydrocarbon tail connected with the small head, it is simply expected to form a highly condensed L film at the air−water interface. Nevertheless, the L film shows a largely expanded state. Mori et al.[18]

CHART 1: Molecular Structure of C_{18}DAO

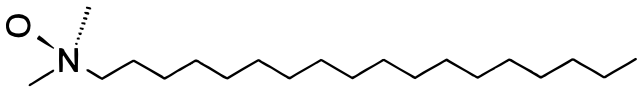

and Myrzakozha et al.[22] reported surface pressure−surface area ($\pi-A$) isotherms of the C_{18}DAO monolayer. By extrapolation of the linear part of the condensed phase in the $\pi-A$ isotherm, the limited surface area is estimated to be ~0.63 nm^2 molecule^{-1}, which is much larger than the cross-section area of a perpendicularly standing molecule. Through atomic-force microscope (AFM) measurements of transferred C_{18}DAO LB monolayers on a mica plate, Mori et al.[18] concluded that the extraordinary expansion of the L film was caused by binding water molecules to the headgroup. The aging effect that reflected water evaporation on a change in AFM image strongly supported this conclusion.

In our previous study,[21] the thermal property of one- and five-monolayer C_{18}DAO LB films, prepared on gold- and silver-evaporated glass slide surfaces, was investigated by infrared reflection−absorption (IRRA) spectrometry. The results show a marked difference in the thermal property between one- and five-monolayer LB films. From the wavenumber shift of C−H stretching vibration bands, it is found that the one-monolayer C_{18}DAO LB film on the gold surface is highly packed with a largely *tilted* stance at room temperature, and it is disordered at 60 °C. The five-monolayer C_{18}DAO LB film on the same substrate, on the other hand, is highly packed with almost *perpendicular* stance at room temperature, and it is largely disordered at 50 °C.

The temperature-dependent wavenumber shift suggests that the first monolayer in a multilayer LB film of C_{18}DAO may be different in thermal property from other layers. The fact that

* To whom correspondence should be addressed. Fax: +81 78 441 7541. E-mail: hasegawa@kobepharma-u.ac.jp.
† Kobe Pharmaceutical University.
‡ Kwansei Gakuin University.
§ Nagoya University.

10.1021/jp992308m CCC: $18.00
Published on Web 11/24/1999

the spectral feature of the monolayer at room temperature is significantly different from that of the multilayer strongly suggests that the discussion of the first layer should be separated from the rest of the layers. This means that the C_{18}DAO multilayers are structurally heterogeneous.

In the previous paper,[21] the fine mechanism of the temperature-induced structural change of the multilayer film was unclear. In the present study, IRRA measurements were performed for the multilayer film, and the structural change was followed quantitatively by a newly proposed method. The new method aims at the investigation of fine insights in the structurally heterogeneous LB film. It is based upon a conventional theory[23] for the analysis of molecular orientation, but the film phase is divided into two phases to distinguish the first layer from other layers. A new thermal property of the C_{18}DAO multilayer LB film was revealed by the new method. In comparison to the results by the conventional theory, the characteristics of the results by the new method are described.

Experimental Section

C_{18}DAO was prepared as previously described.[17] All solvents used were spectroscopic grade and were purchased from Nacalai Tesque Inc. (Kyoto).

Pure water was prepared by an Advantec (Tokyo) automatic water purifier that consists of a deionization column and a double-distillation system. The water subphase in a Langmuir trough was maintained at 20 ± 0.5 °C by a water circulator. The gold-evaporated glass slides for IRRA measurements were cleaned subsequently by pure water, chloroform, and ethanol in a sonicator for 5 min each, followed by the UV−ozone cleaning, before LB depositions.

For $\pi-A$ isotherm measurements and LB film depositions, a chloroform solution of C_{18}DAO (1.0×10^{-3} M) was spread on the surface of pure water in the Langmuir trough to prepare L films. After 30 min was taken to fully evaporate the solvent, the L film was laterally compressed by a Teflon-coated aluminum barrier at a speed of 20 cm^2 min^{-1}. The surface pressure was measured by a Wilhelmy balance. The LB films were prepared by a Kyowa Interface Science Co. Ltd. (Saitama) model HBM LB film apparatus, with the LB (vertical dipping) method.[24] Both dipping and withdrawing speeds of the substrate were 0.5 cm min^{-1}. The transfer ratio was above 0.95 for both dipping and withdrawing. The film structure of the deposited LB films is discussed in an earlier paper.[20]

The LB films deposited on a gold-evaporated glass slide were subjected to IRRA measurements.[25,26] The IRRA measurements were performed at a resolution of 4 cm^{-1} on a Nicolet (Madison, WI) Magna 550 Fourier transform infrared (FT-IR) spectrophotometer equipped with a mercury−cadmium−telluride (MCT) detector at a liquid nitrogen cooled temperature. The number of interferogram accumulations was at least 1000. The p-polarized infrared ray was generated through a JEOL IR-OPT02 wire-grid polarizer. For the IRRA measurements, a Spectra-Tech Inc. (Shelton, CT) specular reflection attachment was used. The angle of incidence was fixed at 80° from the surface normal. The gold-evaporated glass slides for IRRA measurements were purchased from Sinyo Co. Ltd. (Osaka). The thickness of the gold is 300 nm.

For temperature-dependent IRRA measurements, a handmade heating unit that consists of a copper block and a ceramic heater was used. The heating unit was connected with an Omron (Kyoto) E5T programmable temperature controller. The temperature was monitored by a validated copper−constantan thermocouple. The stability of the thermocontroller is within ±0.1 °C.

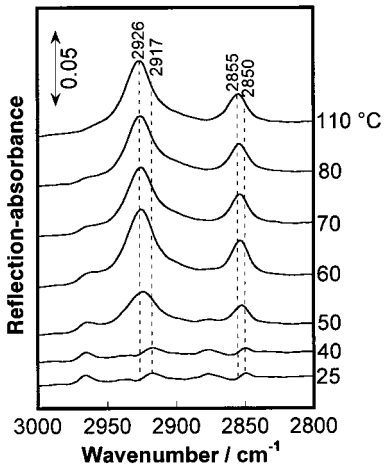

Figure 1. IRRA spectra of the C_{18}DAO seven-monolayer LB film in the temperature range from 25 to 110 °C.

Results

Temperature-dependent IRRA spectra of a seven-monolayer C_{18}DAO LB film deposited on the gold-evaporated glass slide were measured. To emphasize the difference between the first and other layers, seven-monolayer LB films were used instead of the conventional five-monolayer ones.[21] Figure 1 shows a series of spectra of the seven-monolayer C_{18}DAO LB film in the temperature range from 25 to 110 °C. The IRRA spectrum of a dried LB film measured at room temperature (25 °C) was largely different (not shown) from that of the LB film measured before the drying process.[21] The dried LB film proved to have highly ordered molecular packing as compared to those without drying. This change may be caused by self-assembling force, which accompanies full-evaporation of water molecules bound to the film molecules. To remove the drying-induced structural change from the temperature-induced structural change, the IRRA measurements were performed after the sample was dried in a desiccator with P_2O_5 powder at least overnight.

The spectrum in Figure 1 measured at 25 °C shows bands due to the asymmetric and symmetric CH_3 stretching vibrations ($\nu_a(CH_3)$ and $\nu_s(CH_3)$) at 2967 and 2876 cm^{-1}, and those assigned to the antisymmetric and symmetric CH_2 stretching vibrations ($\nu_a(CH_2)$ and $\nu_s(CH_2)$) at 2917 and 2850 cm^{-1}, respectively, accompanied by a Fermi resonance band at 2935 cm^{-1} (very weak). The clear resolution of the CH_3 stretching vibration bands and the Fermi resonance band from the CH_2 stretching vibration bands suggests that the LB film is highly organized at the temperature. This also suggests that the dried LB film has highly organized molecular packing, and molecules are nearly normal to the surface.

It should be noted that the wavenumber shift profile is a little different from that of the five-monolayer LB film that appeared in the previous paper.[21] In the case of the five-monolayer LB film, the $\nu_s(CH_2)$ band is at 2849 cm^{-1} at 25 °C, and it is increased up to 2853 cm^{-1} at 110 °C. In the present case, on the other hand, the band was shifted from 2850 to 2855 cm^{-1} in the same temperature range. This suggests that the film packing was better for the five-monolayer LB film than for the seven-monolayer one. Regardless, the seven-monolayer LB film is still highly organized at the room temperature. The band-intensity profiles for the $\nu_a(CH_2)$ and $\nu_s(CH_2)$ bands against

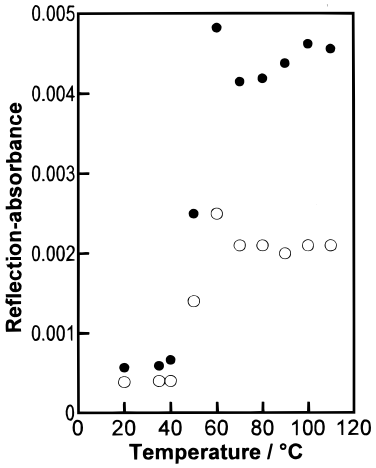

Figure 2. Reflection−absorbance in the RA spectra of the C_{18}DAO seven-monolayer LB film against the temperature of the film. The closed and open circles indicate the intensities of the $\nu_a(CH_2)$ and $\nu_s(CH_2)$ bands, respectively.

temperature are drawn in Figure 2. The profiles show that the low intensities (stable molecular packing) continue until 40 °C. Above 50 °C, however, both band intensities significantly increase. This dramatic increase continues up to 60 °C. The intensity decreases a little at 70 °C, and it does not change largely above 70 °C. Judging from these profiles, the LB film is considered to melt a little above 60 °C.

Discussion

The molecular orientation in the C_{18}DAO LB film built on the gold-evaporated glass slide was estimated by a theoretical method that was established several years ago by Hasegawa, Umemura, et al.[23] The method of molecular-orientation estimation is based on a theory of electric field distribution at an interfacial plane.[27,28] The method can take optical anisotropy of any layers of interest into account in calculation. This enables us to estimate the absorbance (or reflection−absorbance) that depends on molecular orientation, since the anisotropy of the extinction coefficient in a material directly reflects the orientation of transition dipoles at a given wavenumber. With this theory, the molecular orientation is estimated by using observed reflection−absorbance.[23] Details of the calculation will be summarized in the following sections. In the present paper, the observed values appearing in Figure 2 are used for the estimation of the orientation angles.

The optical parameters for the calculation are as follows. The complex refractive indices ($\tilde{n}_j$) of air (phase 1) and the gold layer (phase 3) are $\tilde{n}_1 = 1.0$, and $\tilde{n}_3 = 0.738 + 23.58i$ at 2850 cm^{-1} ($\tilde{n}_3 = 0.711 + 23.08i$ at 2919 cm^{-1}).[29] Here, i is the square root of minus one. The complex refractive indices of the LB film layer (phase 2) consists of two values, $\tilde{n}_o$ and $\tilde{n}_e$, that represent the indices in the direction in-plane (o: ordinary ray) and out-of-plane (e: extraordinary ray). The two values as a function of the orientation angle are used in the optical anisotropic calculation. The real parts of the complex anisotropic refractive indices of the film layer (the second layer) were determined: $n_o = 1.48$ and $n_e = 1.56$.[30] Each anisotropic value, k_o and k_e, is determined by using the extinction coefficient of the bulk sample, k_{bulk}, with the following equations.

$$k_o = \frac{3}{2} k_{bulk} \frac{h_{st}}{h^*_{LB}} \frac{A_{st}}{A_{LB}} \sin^2 \phi \quad (1)$$

$$k_e = 3 k_{bulk} \frac{h_{st} A_{st}}{h^*_{LB} A_{LB}} \cos^2 \phi \quad (2)$$

Here, h^*_{LB}, h_{st}, A_{LB}, A_{st}, and ϕ are the thicknesses of an LB film composed of tilted molecules and a standard LB film of stearic acid, molecular areas of the present LB film and the standard LB film, and the tilt angle of the transition dipole moment discussed, respectively. Each of them will be described in more detail later. The cross-term of h_{st}/h^*_{LB} and A_{st}/A^*_{LB} is newly introduced into the conventional equations[23] to correct molecular packing density, since this cross-term represents a volume-ratio per one molecule between the standard molecule (stearic acid) and C_{18}DAO. For the detail of the original equations, the reader is referred to a previous paper.[23]

In the present study, the extinction coefficients are calculated from those used for LB films of stearic acid by taking the number of methylene groups into account. The extinction coefficient of bulk (powder) C_{18}DAO was estimated from $k_{bulk} = 0.200$[31] for $\nu_s(CH_2)$ at 25 °C by taking the number of methylene groups into account (16 for stearic acid and 17 for C_{18}DAO). The k_{bulk} value of $\nu_s(CH_2)$ of C_{18}DAO was thus estimated to be 0.213 ($0.200 \times 17/16$). The corresponding value of the $\nu_a(CH_2)$ was also determined to be 0.274 by measuring its KBr spectrum (not shown). The bulk extinction coefficient of each band in a spectrum was determined with the use of temperature-dependent KBr infrared transmission spectra. The obtained coefficients of the $\nu_a(CH_2)$ and $\nu_s(CH_2)$ modes are plotted against temperature in Figure 3.

The thickness of a LB film (h^*_{LB}) composed of a hydrocarbon chain with a tilt angle, γ^*, is estimated by eq 3. Here, h_{LB}

$$h^*_{LB} = h_{LB} \cos \gamma^* \quad (3)$$

is the thickness of the LB film where the hydrocarbon chain is assumed to be perfectly normal to the film surface. The approximated tilt angle of the hydrocarbon chain (γ^*) was calculated with the use of the tilt angle (ϕ) of the $\nu_s(CH_2)$ mode. The following approximation equation holds well when the film molecules have uniaxial orientation.[23]

$$\gamma^* = \cos^{-1}(1 - 2\cos^2 \phi)^{1/2} \quad (4)$$

The thickness of each monolayer (h_{LB}) was assumed to be 27 Å,[18] while the standard thickness (h_{st}) was 25 Å.[23] The surface areas (A_{st} and A_{LB}) were estimated from each $\pi-A$ isotherm. The estimated A_{LB} for C_{18}DAO is 42.0 $Å^2$ $molecule^{-1}$. A_{st} is 19.6 $Å^2$ $molecule^{-1}$ that is obtained from our $\pi-A$ isotherm.

In summary, each k_o and k_e is evaluated as a function of ϕ, through γ and h^*_{LB}. The reflection−absorbance is calculated with the k_o and k_e by using the optical anisotropic theory.[23] As a result, the calculation turns out a calibration curve between the reflection−absorbance and orientation angle, ϕ. With the calibration curves for the bands of interest, the molecular orientation angles in the C_{18}DAO LB film were estimated. The results are plotted in Figure 4 against temperature. The estimation was performed only for the temperature range from 20 to 60 °C, since the film melted above 60 °C.

In Figure 4, the calculated tilt angle of the hydrocarbon chain, γ (not γ^*), deduced from the angles of the $\nu_a(CH_2)$ and $\nu_s(CH_2)$ modes is plotted by the closed circles.[23] The figure suggests that the C_{18}DAO LB film is highly organized at around

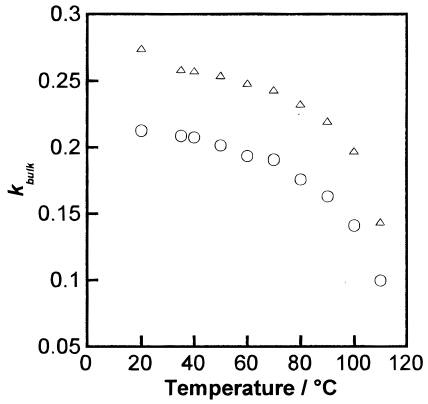

Figure 3. Temperature-dependent extinction coefficients of the bulk samples determined by the KBr pellet measurements. Triangles and circles indicated the coefficients of the $\nu_a(CH_2)$ and $\nu_s(CH_2)$ bands, respectively.

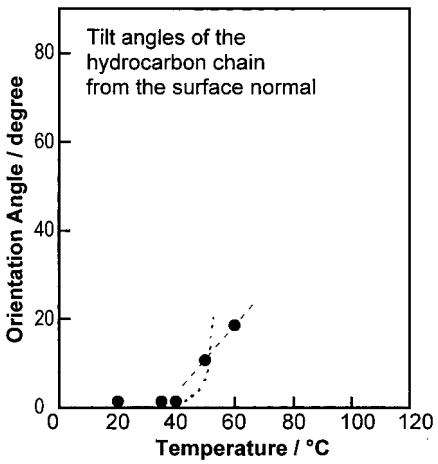

Figure 4. Orientation angles calculated by the three-phase method.

room temperature, and the hydrocarbon chain stands almost normally below 40 °C. The hydrocarbon chain, however, largely tilts above 50 °C. It is of interest that the slope of the increase in γ value is very steep, and the extrapolated line (dashed line) does not smoothly connect to the values below 40 °C. This slope seems a little unnatural. If the increase is simply caused by a dramatic phase transition, the increasing plot is expected to be on a continuous curve that is schematically drawn (dotted curve) in the same figure.

The unnatural increase in the tilt angle reminds us of an interesting result obtained in our previous paper[20] that the film structure of only a monolayer C_{18}DAO LB film is significantly different from that of multilayer LB films. This means that the first layer is largely affected by the interaction with the substrate, which may be largely different from that of film-to-film interaction. In other words, the C_{18}DAO LB films may have heterogeneous film structure where only the first layer has another molecular stance.

To analyze the molecular orientation in the heterogeneous LB film, a new analytical technique was developed and employed. The film phase is divided into two distinct phases for the first and the rest layers. In other words, a four-phase model (IR//air/LB-2/LB-1/Au) is used for the calculation instead of the three-phase model (IR//air/LB/Au) used for Figure 3. Here, LB-1 and LB-2 correspond to the first layer and the rest layers of the LB film phase, respectively (Figure 5).

Each phase of the four-phase model from the air phase to gold phase is simply numbered phase one to phase four,

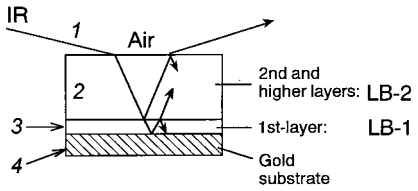

Figure 5. Schematic drawing of the four-phase model that represents the IRRA measurements on a gold-evaporated glass substrate. The film phase is divided into two phases: the first monolayer (LB-1) and other layers (LB-2). The italic figures indicate the number of a phase.

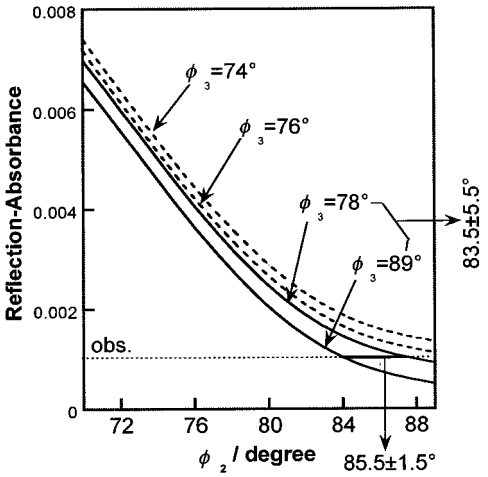

Figure 6. Calculated reflection−absorbance against the orientation angle in phase two, ϕ_2, as a function of the orientation angle in phaes three, ϕ_3.

respectively. The refractive indices of air and gold phases ($\tilde{n}_1$ and $\tilde{n}_4$) are the same as those in the three-phase system ($\tilde{n}_1$ and $\tilde{n}_3$), respectively. Two molecular orientations (ϕ_2, ϕ_3) and two thicknesses (h_2, h_3) are newly introduced for the definition of the complex refractive indices (eqs 1 and 2) of the phases two and three ($\tilde{n}_2$ and $\tilde{n}_3$), respectively. Nevertheless, the two variables (ϕ_2, ϕ_3) could not be estimated simultaneously from only one RA spectrum, since two independent constraints are always necessary to have the two solutions. Therefore, in the present study, solutions with standard deviation are calculated for the estimation of molecular orientation in the two phases.

Figure 6 shows a relation between the calculated reflection−absorbance and ϕ_2 for the $\nu_s(CH_2)$ mode in the seven-layer C_{18}-DAO LB film on the gold-evaporated glass slide. An angle of ϕ_3 (for the first layer) was assumed before calculation. For example, if the observed value is 0.001, the curves of $\phi_3 = 74°$ and 76° do not have a solution (intersection). The curves of $\phi_3 = 83.5 \pm 5.5°$, on the other hand, have intersections with the line at 0.001, and $\phi_2 = 85.5 \pm 1.5°$ is estimated from the figure. The two orientation angles with deviation bars are obtained in this manner. It should be noticed in this example that there is a difference in the average orientation angles in the LB-2 and LB-1 phases. In the same fashion, the orientation angles of the $\nu_a(CH_2)$ mode in the two phases are calculated to obtain the tilt angles in LB-2 and LB-1 phases, γ_2 and γ_3.[23]

The temperature-dependent IRRA spectra of the seven-monolayer C_{18}DAO LB film (Figure 1) were analyzed by the four-phase model calculation. The calculated results are shown in Figure 7. It is found that the LB film at a low temperature shows very small tilt angles from the surface normal for both γ_2 and γ_3 that accompany no deviation. These results are very similar to those obtained by the 3-phase model calculation (Figure 4). This indicates that the adequately dried LB film has a uniformed film structure through the layers where the

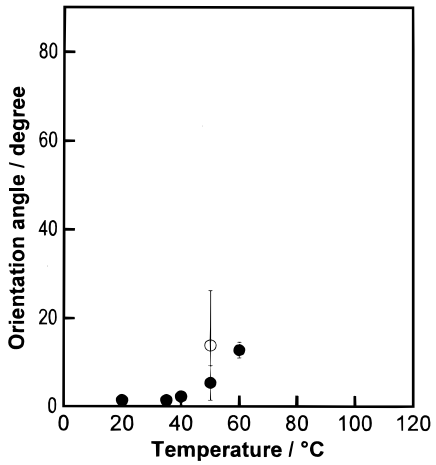

Figure 7. Calculated orientation angles in the C_{18}DAO LB film obtained by the four-phase method. The tilt angle of the hydrocarbon chain, γ, is plotted by open and closed circles, which are for LB-1 and LB-2 phases (i.e., phase three and phase two), respectively.

molecules are highly ordered. This is also supported by a fact that the $\nu_a(CH_2)$ band is resolved from the Fermi-resonance band (2937 cm^{-1}). The $\nu_a(CH_2)$ band is located at 2917 cm^{-1}, which indicates the trans-zigzag conformation of hydrocarbon chain.[32] The calculated orientation angles remain without significant change up to 40 °C, which corresponds to the results in Figure 4.

At 50 °C, however, a remarkable change happens (Figure 7). The average tilt angle in the first layer (LB-1) jumps up to 14°, while the tilt angle in LB-2 phase changes moderately. The deviation bars become large at this temperature especially for the LB-1 phase.

At 60 °C, ϕ_2 was calculated to have a small deviation, as the observed absorbance was very large and contribution of the LB-1 phase to the large absorbance is very small in comparison to that of the LB-2 phase. The angle ϕ_3 could have a large value that is above the magic angle (54.7°), and it was not mathematically confirmed (not shown) for the large absorbance. It is noticed, however, that ϕ_2 by the four-phase model (ca. 11°) is converged fairly well, and it is apparently smaller than that by the three-phase model (ca. 19°) at 60 °C. These results suggest that the LB-1 phase is completely disordered at the temperature, while the LB-2 phase is not perfectly disordered. It can be understood again that the results by the three-phase model are considered to be averaged values of ϕ_2 and ϕ_3. It is of note that the film is not perfectly melted at 60 °C.

An important conclusion revealed by the four-phase model is that the seven-monolayer C_{18}DAO LB film melts *above* 60 °C, while its first layer directly deposited on the substrate starts to be disordered at 50 °C, which is 10 °C lower than the melting temperature at least. It is of interest that the melting and premelting temperatures closely resemble the phase transition temperature of colored (iridescent)-to-turbid solution (49 °C) and that of turbid-to-transparent solution of C_{18}DAO in water (60 °C), respectively.[9] In other words, the thermal property of the multilayer unexpectedly shows similar properties to those of bulk aggregates, and two distinct properties were found in the first and the remaining layers.

The six-monolayer phase laid on the first layer is considered to have bulky property, since the phase comprises crystalline-like molecular aggregates, as compared to the first layer that is directly touched on a gold surface.

Summary

A new method for the estimation of molecular orientation in the structurally heterogeneous LB film was proposed, and it was applied to the temperature-dependent IRRA spectra of the C_{18}DAO LB film.

Although the proposed method was a trial approach, it revealed that the C_{18}DAO LB film consisted of two physically distinguishable phases: the first and other layers. When the temperature of the film was elevated, only the first layer was largely damaged by heating at 50−60 °C, followed by the total melting above 60 °C.

The above study and the previous study of the bulk C_{18}DAO dispersed in water suggest that the thermal property of C_{18}DAO responds to the aggregation form in both bulk and two-dimensional molecular aggregates.

References and Notes

(1) Fields, G. B. *Bioorg. Med. Chem.* **1999**, *7*, 75.

(2) Zanotti, G.; Malpeli, G.; Gliubich, F.; Folli, C.; Stoppini, M.; Olivi, L.; Savoia, A.; Berni, R *Biochem. J.* **1998**, *329*, 101.

(3) Dietrich, C.; Schmitt, L.; Tampe, R. *Proc. Natl. Acad. Sci. U.S.A.* **1995**, *92*, 9014.

(4) Sorgato, M. C.; Moran, O. *Crit. Rev. Biochem. Mol. Biol.* **1993**, *28*, 127.

(5) Engel, A.; Hoenger, A.; Hefti, A.; Henn, C.; Ford, R. C.; Kistler, J.; Zulauf, M. *J. Struct. Biol.* **1992**, *109*, 219.

(6) Okamura, E.; Hayashi, S. *Langmuir* **1999**, *15*, 3589.

(7) Capone, S.; Rella, R.; Siciliano, P.; Vasanelli, L.; Valli, L.; Troisi, L. *Thin Solid Films* **1998**, *327/329*, 465.

(8) Penza, M.; Milella, E.; Anisimkin, V. I. *Sens. Actuators B, Chem.* **1998**, *B47*, 218.

(9) Huo, Q.; Russel, K. C.; Leblanc, R. M. *Langmuir* **1998**, *14*, 2174.

(10) Owen, D. J.; Evans, P. R. *Science* **1998**, *282*, 1327.

(11) Handa, T.; Nakagaki, M. *Adv. Colloid Interface Sci.* **1992**, *38*, 45.

(12) Saito, H.; Miyako, Y.; Handa, T.; Miyajima, K. *J. Lipid Res.* **1997**, *38*, 287.

(13) Hasegawa, T.; Kawato, H.; Toudou, M.; Nishijo, J. *J. Phys. Chem. B* **1997**, *101*, 6701.

(14) Blume, A.; Hubner, W.; Messner, G. *Biochemistry* **1988**, *27*, 8239.

(15) Weck, M.; Fink, R.; Ringsdorf, H. *Langmuir* **1997**, *13*, 3515.

(16) Koyano, H.; Bissel, P.; Yoshihara, K.; Ariga, K.; Kunitake, T. *Chem. Eur. J.* **1997**, *3*, 1077.

(17) Imae, T.; Sasaki, M.; Ikeda, S, A. *J. Colloid Int. Sci.* **1989**, *131*, 601.

(18) Mori, O.; Imae, T. *Langmuir* **1995**, *11*, 4779.

(19) Imae, T.; Tsubota, T.; Okamura, H.; Mori, O.; Takagi, K.; Itoh, M.; Sawaki, Y. *J. Phys. Chem.* **1995**, *99*, 6046.

(20) Myrzakozha, D. A.; Hasegawa, T.; Imae, T.; Nishijo, J.; Ozaki, Y. *Langmuir* **1999**, *15*, 3595.

(21) Myrzakozha, D. A.; Hasegawa, T.; Imae, T.; Nishijo, J.; Ozaki, Y. *Langmuir* **1999**, *15*, 3601.

(22) Myrzakozha, D. A.; Hasegawa, T.; Imae, T.; Nishijo, J.; Ozaki, Y. *Surf. Sci.*, in press.

(23) Hasegawa, T.; Takeda, S.; Kawaguchi, A.; Umemura, J. *Langmuir* **1995**, *11*, 1236.

(24) Blodgett, K. B. *J. Am. Chem. Soc.* **1934**, *56*, 495.

(25) Greenler, R. G. *J. Chem. Phys.* **1966**, *44*, 310.

(26) Takenaka, T.; Umemura, J. *Vibrational Spectra and Structure Vol. 19*; Durig, J. R., Ed.; Elsevier Science Publishing; Amsterdam, 1991; p 215.

(27) Hansen, W. N. *J. Opt. Soc. Am.* **1968**, *58*, 380.

(28) Drude, P. *Ann. Phys. U. Chem. N. F.* **1889**, *32*, 584.

(29) Ordal, M. A.; Long, L. L.; Bell, R. J.; Bell, S. E.; Bell, R. R.; Alexander, R. W., Jr.; Ward, C. A. *Appl. Opt.* **1983**, *22*, 1099.

(30) Paudler, M.; Ruths, J.; Riegler, H. *Langmuir* **1992**, *8*, 184.

(31) Popenoe, D. D.; Stole, S. M.; Porter, M. D. *Appl. Spectrosc.* **1992**, *46*, 79.

(32) Senak, L.; Moore, D.; Mendelsohn, A. *J. Phys. Chem.* **1995**, *96*, 2749.